Available online at www.sciencedirect.com

SciVerse ScienceDirect

Surface Science Reports 67 (2012) 233–243

surface science reports

www.elsevier.com/locate/surfrep

Trace elemental analysis by laser-induced breakdown spectroscopy—Biological applications

Jozef Kaiser[a,f,*], Karel Novotný[c,f], Madhavi Z. Martin[d], Aleš Hrdlička[f], Radomír Malina[a,f], Martin Hartl[b], Vojtěch Adam[e,f], René Kizek[e,f]

[a]Institute of Physical Engineering, Faculty of Mechanical Engineering, Brno University of Technology, Technická 2896/2, 616 69 Brno, Czech Republic
[b]Institute of Machine and Industrial Design, Faculty of Mechanical Engineering, Brno University of Technology, Technická 2896/2, 616 69 Brno, Czech Republic
[c]Department of Chemistry, Faculty of Science, Masaryk University, Kotlářská 2, 611 37 Brno, Czech Republic
[d]BioSciences Division, Oak Ridge National Laboratory, Oak Ridge, TN 37831, USA
[e]Department of Chemistry and Biochemistry, Mendel University in Brno, Zemědělská 1, 613 00 Brno, Czech Republic
[f]Central European Institute of Technology, Brno University of Technology, Technická 3058/10, CZ-616 00 Brno, Czech Republic

Received 24 February 2011; received in revised form 31 March 2011; accepted 28 August 2012
editor: W. H. Weinberg
Available online 17 November 2012

Abstract

Laser-Induced Breakdown Spectroscopy (LIBS) is a sensitive optical technique capable of fast multi-elemental analysis of solid, gaseous and liquid samples. Since the late 1980s LIBS became visible in the analytical atomic spectroscopy scene; its applications having been developed continuously since then. In this paper, the use of LIBS for trace element determination in different matrices is reviewed. The main emphasis is on spatially resolved analysis of microbiological, plant and animal samples.

Keywords: Laser-induced breakdown spectroscopy; LIBS; Mapping; Trace elements; Phytoremediation; Cancer; Plant; Bacteria; Animal tissues

1. Introduction

Laser-Induced Breakdown Spectroscopy (LIBS) is an established analytical technique based on spectroscopic analysis of radiation, which is emitted by a micro-plasma induced on the analyte surface by a laser pulse. The relative simplicity of the LIBS principle makes this technique very attractive for a large variety of applications [1–3]. The first analytical use of laser plasma on surfaces and hence the birth of LIBS is dated to 1962–1963 [4,5]. Up to the 1980s, the lasers were used mainly for sampling to another excitation source, i.e. to vaporize a small amount of sample for analysis, e.g. by the conventional electrode spark [1,6]. The instrumentation development in plasma diagnostics in the 1970s resulted in modern detectors that allowed electronic gating and averaging of the signals from the plasmas [7]. The development of relatively compact, highly energetic laser sources in the early 1980s, together with further improvements in detector capabilities and a decrease in the size and price of LIBS components, caused LIBS applications to significantly grow in number and variety.

The term LIBS was originally used for time integrated measurements in 1981 [8]; earlier this technique was also called Laser-Induced Plasma Spectroscopy (LIPS), Laser Spark Spectroscopy (LSS) or Laser Optical Emission Spectroscopy (LOES) [1]. Time-Resolved LIBS measurements, which are nowadays most commonly used, were formerly quoted TRELIBS [9]. Currently LIBS is the term used for all above-mentioned methods.

The theoretical background of LIBS has already been overviewed in several monographs [1–3] and articles [10,11]. Hahn and Omenetto presented [10], in the first

*Corresponding author at: Institute of Physical Engineering, Faculty of Mechanical Engineering, Brno University of Technology, Technická 2896/2, 616 69 Brno, Czech Republic. Tel.: +420 5 4114 2846; fax: +420 5 4114 2842.
E-mail address: kaiser@fme.vutbr.cz (J. Kaiser).

0167-5729/$ - see front matter © 2012 Elsevier B.V. All rights reserved.
http://dx.doi.org/10.1016/j.surfrep.2012.09.001

part of their review, various topics and techniques used for the spectroscopic characterization of plasmas [10]. Diagnostic approaches such as the measurement of atomic and ionic emission, absorption and fluorescence, scattering methods and many theoretical expressions relating the emission signal to the plasma parameters have been given (measurement of line intensity, line profiles, ion-to-neutral ratios and line-to-continuum ratio). Application of these expressions to the evaluation of electron number density and plasma temperature has been shown. It has also been concluded that the time scale for the diffusion of heat (from the plasma to the particle) and mass (from the particle to the plasma) govern the overall plasma conditions. In the second part [11] they focused on quantitative LIBS analysis describing various calibration strategies with respect to many matrix interferences. Mathematical expressions were also given and any field of LIBS action was included. Tognoni et al. [10] reviewed the experimental approaches for obtaining quantitative micro analysis using the LIBS technique. The authors discuss in detail the influence of laser power, wavelength, pulse length, laser beam profile, choice of experimental geometry, importance of ambient gas choice and the role of detectors for improving the precision of LIBS analysis. The LIBS fundamentals, together with the instrumentation, different LIBS applications and future trends are discussed by Pasquini et al. [11]. Tognoni et al. [12] described Calibration-Free LIBS (CF-LIBS), i.e. multi-elemental quantitative analysis of LIBS spectra. This approach is based on the measurement of line intensities and plasma properties (plasma electron density and temperature) and on the assumption of a Boltzmann population of excited levels which does not require the use of calibration curves or matrix-matched standards. The first part of this critical review is focused on CF-LIBS applications. Quantitative results reported in the literature, obtained in the analysis of various materials and in a wide range of experimental conditions, are then summarized with a special emphasis on nominal composition values. In the second part, the simplifying assumptions, which lie at the basis of the CF-LIBS algorithm, are discussed (stoichiometric ablation and complete atomization, thermal equilibrium, homogeneous plasma, thin radiation, detection of all elements). Xian-Yun Liu and Wei-Jun Zhang [13] reviewed the potential application of LIBS in the biomedical field, including bio-aerosol detection and identification, tissue and mineral analysis in the human body. Cremers and Chinni [14] overviewed the LIBS methods as an analytical technique, together with their capabilities and limitations, including a discussion on how these features relate to potential applications. LIBS achievements in the analysis of various kinds of artwork, cultural heritage samples including buildings and objects of various kinds, soils, meteorites and space objects are reviewed by Gaudiuso et al. [15]. Recent developments in LIBS industrial applications have been summarized in the work of Bol'shakov et al. [16].

In this paper, the utilization of LIBS for trace element analysis in different biological matrices with the main emphasis on the trace elemental mapping in biological samples is reviewed.

2. LIBS principles of trace element analysis and mapping

The result of elemental mapping is the information about the element line intensity (or area) versus one or more spatial coordinates. The images of the spatial distribution serve to establish compositional interrelationships of the elemental constituents in the sample.

Laser-assisted sampling of various samples resulted in the development of what is nowadays a routinely used analytical technique known as Laser Ablation Inductively Coupled Plasma Optical Emission Spectrometry or Mass Spectrometry (LA-ICP-OES/MS) [17]. Comparing LIBS to LA-ICP-OES/MS highlights that the LIBS setup is simpler and in general terms more cost effective [18]. Considering the capabilities of spatially-resolved analysis, LIBS gives an instantaneous signal directly related to the location at which a single ablation event occurred. On the contrary, mapping using LA-ICP-OES/MS usually brings more experimental difficulties since it involves sample transport and inevitable sample dispersion in the ablation chamber and in the tubing. This means that, without considerable care, the signal produced in the mass (or optical) spectrometer is not directly attributable to a specific location on the sample [19]. On the other hand, when using LIBS as a full, quantitative, fast-scanning on-line technique to characterize various samples in the field of material sciences, the main problem of matrix dependent quantification procedures has to be overcome [20]. It should be also noted that LIBS analytical outcomes may be influenced by the re-deposition of materials on the surface, if no buffer gas flow is used.

Resolution of the surface resolved analysis is influenced not only with the beam spot size on the sample surface or the distances of ablation craters. It can be defined as the smallest distance between two ablation spots on which any potential changes in composition can be registered at a certain level of significance. The term 'lateral resolution' is most frequently used. However, in the 2D surface analysis community, different definitions of lateral resolution are in use and there is no generally accepted method for its determination [21]. Lateral resolution is generally influenced by (a) the beam diameter on the sample surface, (b) the laser pulse energy, (c) the laser pulse duration, (d) the material properties of the sample and (e) the type and pressure of the ambient gas atmosphere [22]. Using low-energy, short wavelength or short pulse-duration (ps, fs) laser pulses, ablation craters with micron scale sizes laterally and nm scale sizes in depth can be produced [3]. It should be also noted that the detection region, which is ionized sufficiently to yield emission signals, and the total region, which is ablated by the laser pulse, may be considerably different. It holds true for ns ablation where part of the ablated material is removed after the laser pulse by

the shock wave and melt wave propagating into the target. The crater size will therefore represent an upper boundary to the actual region probed in composition measurements [3].

It should be highlighted that the LIBS mapping weakness, similarly to other Laser-Ablation based techniques, is mainly the correct selection and adjustment of the laser focusing optics. The used laser wavelength has to be taken into consideration in order to produce a matrix of ablation craters with an appropriate spatial resolution [10,11]. Small ablation craters (3 μm) can be created even with the fundamental Nd:YAG wavelength (1064 nm) by applying a focusing objective with a high numerical aperture (0.45), short focal length (19 mm), laser beam expander and 0.1 mJ pulse energy [23,24]. Such small craters are particularly suitable for selected applications of LA-ICP-MS [25,26] providing better sensitivity than LIBS. LIBS mapping is usually performed with 10 μm in diameter (or wider) craters; up to about 20–30 μm is called micro LIBS [10,23,27]. It is worth mentioning that most theoretical studies published on this topic were done with metallic or glass reference materials [10,23]. This is very understandable due to the well-defined structure and composition of these materials.

The current choice of laser instrumentation on the market enables the production of ablation craters from units of micrometers; this is on a par with the spatial resolution of particle beam—based methods [24,28]. However, the production of craters as small as possible brings about a low amount of ablated material. Moreover, the small microplasma volume cools down quickly and thus cannot excite a sufficient number of analyte atoms. As a result, a weaker LIBS emission signal with a poor signal—to—noise (S/N) ratio is obtained [23]. Real biological samples can profit from a combination of good lateral and depth resolution. Besides, it is obvious that Limit of Detection (LOD) should be sufficiently lower than the trace concentration levels of the determined elements. In some specific cases, the total ablation depth is also very important when approaching the depth resolution comparable with the cell wall [29]. The accomplishment of these conflicting requirements can be considered as the main task of the elemental mapping of biological samples with LIBS. When reaching the lateral resolution in the order of units of μm, LIBS can replace other microanalytical methods except for Secondary Ions Mass Spectrometry (SIMS) [24,28] and high-brilliance synchrotron powered micro X-ray Fluorescence Spectroscopy (μ–XRF) [28,30]. Among them, Electron Microprobe X-ray Microanalysis (EPXMA) is rarely used in biology [31]. On the other side, SIMS can be used for sub-micrometric elemental analyses, e.g. analysis of subcellular components with much more complicated and expensive instrumentation in comparison with LIBS [26,28]. For mapping of biomolecule distributions, Matrix-Assisted Laser Desorption/Ionization (MALDI) can be used [26]. The achievable lateral resolution is 15 μm in a nanoparticle Assisted Laser Desorption/Ionization (nano-PALDI) modification [26,32]. The submicrometric lateral resolution is also feasible by applying so-called near field LA, although with a poor emission yield [24,25]. The reported lateral resolution down to 50 nm is compatible with MS detection [25].

LIBS is capable of light-element detection, useful for material identification, depth profiling and elemental surface mapping, so it can solve numerous industrial and scientific problems in real-time [11–16,33]. On the other hand, LIBS LODs, which in its basic configurations are typically of the order of mg kg^{-1} or tens of mg kg^{-1}, are poorer with respect to other more traditional analytical techniques for most of the elements. However, it should be also noted that the LIBS LODs can be improved by applying modified LIBS techniques such as Double-Pulse (DP) LIBS or combining laser ablation with Laser-induced Fluorescence spectrometry (LIFS) [2,33]. An improvement of S/N ratio over an order of magnitude can be realized by reheating the existing microplasma with a second laser pulse (DP LIBS). This approach is advantageous in terms of lower sample load [1,2,34]. DP LIBS ablation craters can be acceptably small and comparable with those from LA-ICP-MS for e.g. elemental mapping [35,36]. Another method for improving S/N is a combination LA and LIFS, which is capable of a selective re-excitation of particular analyte atoms by a second laser pulse, the wavelength of which precisely corresponds to an atomic transition of the element [37].

3. Selected biological LIBS applications

3.1. LIBS analysis of cells and microorganisms

Analysis of cells, sub-cellular components and individual microorganisms with optical methods requires a specific high level of resolution. Meur et al. [38] developed a method to detect and quantify label-free nucleic acids by stoichiometric proportioning of phosphorous in the nucleic acid skeleton using μLIBS and a specific statistical analysis, which indicated the error probability for each measurement. Their report on quantitative results with a limit of detection of 10^5 nucleotides/μm^2 (i.e. 2×10^{13} phosphorus atoms/cm^2) has been documented. Initial micro-array analysis has given very encouraging results, which point to new ways of quantifying hybridized nucleic acids.

In general, the application of LIBS to bacterial and animal samples is still not common and hence make it cutting edge; however, the advantage of LIBS is a predisposition for wider employment of this technique. As far as the number of articles is concerned, LIBS is more commonly used for the analysis of bacterial samples compared to animal tissues. LIBS is generally used for quantification of various elements in microorganisms. These results are then statistically processed to find a way to distinguish between various microorganism species according to the content of target elements. On the other hand, some authors show that LIBS can be used for the rapid analysis of potential hazardous materials to find the presence of

microorganism. First such applications were published in 2003 by Morel et al. [39] and Samuels et al. [40]. The first mentioned group analyzed six bacteria and two spores species in pellet form. The intensity ratio as a quantitative criterion was optimized because of its linearity and reproducibility. Under the published experimental conditions TRELIBS exhibited a good ability to differentiate among all of the species, whatever the culture medium, the species or the strain was. The second group utilized LIBS for distinguishing between bacterial spores, molds, spores, and proteins. The biosamples were prepared and deposited onto porous silver substrates. LIBS data from the individual laser shots were analyzed by principal-component analysis and were found to contain adequate information to afford discrimination among the different biomaterials.

One year after the first publication on LIBS for analysis of bacterial samples, another work was reported [41], where the authors used LIBS for recording the plasma emission for the colonies of vegetative cells or spores of five bacterial strains: *Bacillus thuringiensis* T34, *Escherichia coli* IHII/pHT315, *Bacillus subtilis* 168, *Bacillus megaterium* QM B1551, and *Bacillus megaterium* PV361. The major inorganic components of the bacterial samples, including Ca, Mn, K, Na, Fe and phosphate, were clearly detected. The authors again demonstrated the ability of LIBS to easily distinguish bacterial strains according to their different accumulation of various elements.

In 2006, Baudelet et al. published three papers aimed at using LIBS for bacteria analysis. Primarily, they showed the applicability of fs LIBS for the analysis of *Escherichia Coli* and *Bacillus subtilis* [42]. The obtained spectra were compared with those resulting from the ns LIBS. Specific features of fs LIBS have been demonstrated, which make this technique very attractive for analyzing biological samples: (i) lower plasma temperature leading to negligible nitrogen and oxygen emissions from the excited ambient air and a better contrast in detection of trace mineral species; and (ii) specific ablation regime that favors intramolecular bond emissions with respect to atomic emissions. A precise kinetic study of molecular band head intensities allowed the authors to distinguish the contribution of native CN bonds released by the sample from that due to carbon recombination with atmospheric nitrogen. This phenomenon was confirmed and studied in greater depth in other papers published by the same group [43]. Finally, they confirmed the ability to use LIBS as a bacterial-strain-distinguishing tool on the analysis of five different analyzed species of bacterium [44]. It was found that the concentration profile of trace elements allowed unambiguous discrimination of different bacteria. Quantitative differentiation has been made by representing bacteria in a six-dimensional hyperspace with each of its axis representing a detected trace element. In such a hyperspace, representative points of different species of bacterium were gathered in different and distinct volumes.

Diedrich et al. [45] demonstrated the advantages of LIBS on the analysis of a pathogenic strain of bacteria, *Escherichia coli* O157:H7 and compared the results obtained with three nonpathogenic *Escherichia coli* strains: a laboratory strain of K-12, a derivative of the same strain termed HF4714 and an environmental strain, *Escherichia coli* C. A discriminant function analysis (DFA) was performed on the LIBS spectra obtained from the live colonies of all four strains. Utilizing the emission intensity of 19 atomic and ionic transitions from trace inorganic elements, the DFA revealed significant differences between pathogenic and non-pathogenic strains, suggesting the possibility of identifying and discriminating the pathogenic strain from commonly occurring environmental strains. The same authors also determined various spectra depending on bacteria strain, which enabled them to distinguish between *Escherichia coli* strains and one strain of environmental mold, as well as one strain of *Candida albicans* yeast [46]. In order to find the influence of various compositions of media used for the cultivation of bacteria, LIBS was applied to analyze *Pseudomonas aeruginosa* bacterial colonies cultivated in the presence of a Trypticase Soy Agar (TSA) plate, a blood agar plate, and a medium chosen deliberately to induce bacterial membrane changes, a MacConkey agar plate containing bile salts [47].

The results from the previous study were confirmed and extended in the paper by Rehse et al. [48] who also used LIBS to distinguish between two different genera of gram-negative bacteria and also between several strains of the *Escherichia coli* bacterium based on the relative concentration of trace inorganic elements in the bacteria. From the point of view of LOD as a count of cells, the same authors demonstrated that specimens with a reduced number of bacterial cells (approximately 2500) were identified with 100% accuracy when compared to undiluted specimens [49].

LIBS was also successfully tested on blind samples of bacterial pathogens, both species and strain [50]. The pathogens used for the study were chosen and prepared by one set of researchers. The LIBS data were collected and analyzed by another set of researchers. The latter researchers had no knowledge of the sample identities other than that (a) the first five of fifteen samples were unique (not replicates), and (b) the remaining ten samples consisted of two replicates of each of the first five samples. Using only chemometric analysis of the LIBS data, the ten replicate bacterial samples were successfully matched to each of the first five samples. The results of this blind study show that it is possible to differentiate the bacterial pathogens *Escherichia coli*, three clonal methicillin-resistant *Staphylococcus aureus* (MRSA) strains, and one unrelated MRSA strain using LIBS.

LIBS also enables the analysis of samples from various distances *in situ*. From the technological point of view, the group of Miziolek et al. [51,52] developed a double-pulse Standoff Laser-Induced Breakdown Spectroscopy (ST-LIBS) system capable of detecting a variety of hazardous materials at tens of meters. Amongst others, the experimental setup was used to detect anthrax surrogate *Bacillus subtilis* and chemical warfare agents at distances of 20 m. Concerning warfare agent detection, the detection and discrimination of

the biological warfare agent surrogates *Bacillus subtilis* (also known as *Bacillus globigii*, or BG) (2% false negatives, 0% false positives) and ovalbumin (0% false negatives, 1% false positives) at 20 m using ST-LIBS and linear correlation was demonstrated [52]. Unknown interfering samples (not included in the model), samples on different substrates and mixtures of BG and Arizona road dust were classified with reasonable success using partial least squares discriminant analysis.

Lewis et al. [55] used fs LIBS combined with chemometric (Principal Component Analysis and Partial Least Squares) analysis to differentiate and discriminate among bacteria from the unmined and rehabilitated bauxite soils. Lines of Ca, Mg, K Na and Zn were mainly used for statistical processing. This approach can be utilized not only to discriminate between inter-and intra-site differences in the soil bacteria but also for differentiating both bacterial species and strain. The identification of the soil bacteria was limited to phylogenetic analysis. The bacteria sample was a microscope glass slide on which a bacteria colony was evenly smeared.

3.2. LIBS analysis of animal tissues

In addition to bacterial research, human and animal tissues are other biological samples which are of interest for LIBS [53]. Cancer diagnosis and classification is extremely complicated and, for the most part, relies on subjective interpretation of biopsy material. Such methods are laborious and in some cases might result in different interpretations depending on the histopathologist doing the examination. Automated, real-time diagnostic procedures would greatly facilitate cancer diagnosis and classification. In 2004 LIBS was used for the first time to distinguish between normal and malignant tumor cells from dog histological sections by Kumar et al. [54]. It was found that the concentration of trace elements in normal and tumor cells was significantly different. El-Hussein et al. followed this direction by an *in vitro* study of using LIBS as a quick and simple method for spectrometric analysis to identify and characterize some types of human malignancies [55]. This was performed via detection of the abundance of certain elements—namely calcium and magnesium—in malignant tissues with respect to the non-neoplastic ones. In order to improve the performance of the LIBS technique, measurements have been performed under vacuum and the samples were frozen down to -196 °C in a specially designed vacuum chamber. Under such experimental arrangements, a pronounced enhancement was achieved in the S/N ratio of different spectral lines. Significant discriminating results have been obtained in the case of breast and colorectal cancers indicating the possibility of adopting LIBS in the early detection of malignancy as well as the identification of the severity and grade of the disease. In addition, Myers et al. showed a portable LIBS system as a capable tool for real-time material analysis without sample preparation [56]. Nevertheless, all published papers are aimed at the determination of elements and not on mapping, which is still a challenge.

Besides malignancies, Santos et al. evaluated the performance of fs LIBS for the determination of elements in animal tissues [57]. Sample pellets were prepared from certified reference materials, such as animal liver, kidney, muscle and hepatopancreas and oyster, after cryogenic grinding assisted homogenization. Data obtained indicated that it was both a matrix-independent sampling process and that fs LIBS could be used for the determination of Ca, Cu, Fe, K, Mg, Na, and P, but efforts had to be made to obtain more appropriate detection limits for Al, Sr, and Zn. Moreover, LIBS was also utilized for the analysis of chicken brain, lung, spleen, liver, kidney and skeletal muscle [58]. Different data processing techniques were used to study whether the information contained in these LIBS spectra was able to be differentiated between the various types of tissue samples and then identify unknown tissues. The authors demonstrated an ability to clearly distinguish between each of the known tissue types with only 21 selected analyte lines from each observed LIBS spectrum.

3.3. LIBS analysis of plant samples

Metals play an important role in plant function and metabolism. The transport and localization of these elements within the different plant parts is critical for understanding metabolic pathways. The resultant knowledge concerning metal distribution can be applied to plant physiology, agricultural research, food science and genetic engineering. A recent review on "conventional" *in situ* techniques to visualize spatial distributions and assess the speciation of metals and metalloids was published by Lombi et al. [59]. The techniques addressed in this review included: histochemical analysis, autoradiography, LA-ICP-MS, SIMS, SEM (including EDX), PIXE and synchrotron methods i.e. XRF, differential and fluorescence tomography, and X-ray absorption techniques. Even though LIBS had already been proven to be a comparable tool for mapping, it was not included. Another recent review by Santos et al. focused on both bulk and spatially resolved LIBS analyses of plant samples [63]. Among others, a chapter on quantitative LIBS analysis of plants was presented. Therefore, here the selected LIBS applications for elemental mapping of plant samples are reviewed. Table 1 summarizes the LIBS studies on plant samples, microorganisms and animal tissues. Together with the investigated species, the elements studied and the appropriate references are given.

The group of Martin et al. [60] used LIBS for high resolution applications in the elemental analysis of a variety of environmental samples and as a proof of concept for a host of forensic applications. It has been demonstrated that LIBS in combination with multivariate analysis can be employed e.g. to analyze the chemical

Table 1
LIBS study on plant samples, microorganisms and animal tissues. Together with the investigated species, the elements studied and the appropriate references are given.

Species	Elements	Refs.
Plants		
Bermuda grass (*Cynodon dactylon*)	Al, Ca, C, Mg, Si, Sr, Zn	[67]
Brachiaria (*Brachiaria decumbens*)	B, Cu, Fe, Mn, Zn	[71]
Boldo (*Pneumus boldus*)	B, Cu, Fe, Mn, Zn	[71]
Pepper (*Capsicum annuum*)	Pb, Mn, K	[66]
Coffee (*Coffea arabica*)	B, Cu, Fe, Mn, Zn	[71]
Endive (*Cichorium endivia*)	B, Cu, Fe, Mn, Zn	[71]
Grass (*Axonopus obtusifolius*)	B, Cu, Fe, Mn, Zn	[71]
Jack (*Artocarpus integrifolia*)	B, Cu, Fe, Mn, Zn	[71]
Lettuce (*Lactuca sativa*)	B, Cu, Fe, Mn, Zn	[71]
Longleaf pine (*Pinus palustris*)	Ca, Fe, Na, S	[60]
Maize (*Zea mays*)	B, Cu, Fe, Mn, Zn	[71]
Mango (*Mangifera indica*)	B, Cu, Fe, Mn, Zn	[71]
Oranges (*Citrus sinensis*)	Ca, C, Cl, H, Fe, Mg, Mn, Ni, N, O, K, S, Na, Zn	[73]
Pepper (*Piper nigrum*)	B, Cu, Fe, Mn, Zn	[71]
Potato (*Solanum tuberosum*)	Al, Ba, Be, Ca, C, Cl, Cr, Co, Cu, H, Fe, Li, Mg, Mn, Mo, Ni, N, O, K, Rb, Si, Na, Sr, S, Ti, V	[68,69]
Red Osier Dogwood (*Cornus stolonifera*)	Fe	[74]
Sophora (*Styphnolobium japonicum*)	Ca	[66]
Soya (*Glycine max*)	B, Cu, Fe, Mn, Zn	[71]
Spinach (*Spinacia oleracea*)	Ca, Mg, P, B, Cu, Fe, Mn, Zn, Al, Si	[70]
Sunflower (*Helianthus annuus*)	Ca, Cu, Pb, Mn, Mg, K, Ag	[29,62–65]
Tall fescue (*Festuca arundinacea*)	Cd, Ca, Fe, Pb, Mn, Mg, Zn	[61]
Microorganisms		
Alternia alternata	Al, Cr, Cu, Au, In, Pb, Ag	[51]
Bacillus cereus	Ca, C, Mn, Ag	[40]
Bacillus megaterium	Ca, Fe, Mn, K, Na	[41]
Bacillus subtilis	Al, Ca, C, Cr, Cu, H, Au, In, Fe, Pb, Mg, Mn, N, K, Ag, Na	[39–42,51,52]
Bacillus thuringiensis	Ca, C, Fe, Mg, Mn, K, Ag, Na	[39–41]
Candida albicans	Ca, C, Mg, P, K, Na	[46]
Escherichia coli	Ca, C, Cl, H, Fe, Mg, Mn, N, O, P, K, Na	[39,41,42, 44–46,48–50]
Mycobacterium smegmatis	Ca, C, Mg, P, Na	[49]
Proteus mirabilis	Ca, Mg, K	[39]
Pseudomonas aeruginosa	Ca, C, Mg, P, Na	[47,48]
Stachybotrys chartarum	Ca, C, Mg, P, K, Na	[46]
Staphylococcus aureus	Ca, C, Mg, P, K, Na	[39,49,50]
Staphylococcus saprophyticus	Ca, C, Mg, P, Na	[49]
Streptococcus mutans	Ca, C, Mg, P, Na	[49]
Streptococcus viridans	Ca, C, Mg, P, Na	[49]
Animal tissues	Al, Ca, Cu, Fe, Mg, K, Na	[54]
Hemangiosarcoma and normal liver tissues; dog (*Canis lupus familiaris*)		
Breast and colorectal carcinoma tissues; human (*Homo sapiens*)	Ca, Mg	[55]
Mammalian liver, kidney, muscle and hepatopancreas, and oyster	Al, Ca, Cu, Mg, Fe, P, K, Na, Sr, Zn	[57]
Brain, lung, spleen, liver, kidney and muscle; chicken (*Gallus gallus domesticus*)	Al, Ca, C, Cr, Cu, Fe, Li, Mg, Mo, Ni, P, K, Sc, Sr, Na, Zn	[58]

composition of annual tree growth rings and correlate them to external parameters such as changes in climate, forest fires, and disturbances involving human activity. The objectives of using LIBS in fire scar determinations are (1) to determine the characteristic spectra of wood exposed to forest fires, and (2) to examine the validity of this technique for detecting fire occurrences in tree trunks that did not develop fire scars. These examples demonstrate that the LIBS-based techniques are inherently well suited for diverse environmental applications. LIBS was also used by the same authors to determine the impact of endophyte (*Neotyphodium* sp.) infection on elemental composition of tall fescue (*Festuca arundinacea*) [61]. Particularly, LIBS has been successfully used to detect Fe, Mn, Mg, Pb, Ca, Zn, and Cd in the tall fescue leaf tissue samples. However, the insufficient number of samples precluded unequivocal determination of the presence of a common endophyte affected by the concentration of metals in the leaf tissue. Advances in LIBS applications could benefit forage quality studies and phytoremediation research because LIBS allows trace metal analysis at low cost both in the field and in near real time.

Bossu et al. [66] revealed a surface contamination of Sophora leaves with Ca brought about by air pollution but the spectra were averaged from 5 shots on the upside of each leaf. They used a fs Ti: Saphire 800 nm laser, however, ns Nd:YAG laser emitting its second harmonic wavelength 532 nm is frequently used as in Chauhan et al. [67]. Herein Si in the different parts (leaf blade, leaf sheath and stem) of Bermuda grass (*Cynodon dactylon*) was monitored. Silicon protects plants from diseases and is concentrated in cells called as phytolits. The enhanced Si concentration was correlated with the phytolits distribution. A higher concentration was found in leaf blades than in leaf sheaths and stems.

The group of Kaiser et al., Novotný et al. and Kizek et al. [62–66] used LIBS in their research as one of the methods to map the elemental distribution in plant compartments of different plant species. The results of LIBS and LA-ICP-MS analysis were compared with the outcomes from Atomic Absorption Spectrometry (AAS) and Thin-Layer Chromatography (TLC). They proved

LIBS capability for the fast analysis of large area (cm × cm) samples with a spatial resolution up to 200 μm. In their recently published paper [66], LIBS and LA-ICP-MS have been applied for high-resolution 2D mapping of accumulation and distribution of a heavy metal (Pb) and nutrition elements (K, Mn) in leaves of *Capsicum annuum* L. samples. Elemental mapping performed on fresh (frozen) and dried leaves was compared.

Martelli et al. [67] reported on a new methodology based on pulsed lasers in order to estimate wheat outer layer mechanical properties without sample preparation. Laser experiments were carried out with an Argon Fluoride ($\lambda = 193$ nm, 15 ns pulse duration) excimer laser source. Wheat grains from two cultivars were irradiated by single laser pulses with a quasi-uniform irradiation and two intensities (2.5 J cm^{-2} and 5 J cm^{-2}). The ablation flux was characterized by environmental scanning electron microscopy before measuring the removed material on cross-sections observed by confocal scanning laser microscopy. Specific image treatment was carried out to obtain the ablation flux (amount of removed matter per pulse). The pericarp, seed coat and aleurone layer were gradually ablated under the laser conditions used. Their ablation thresholds were different and could be related to tissue cohesion. Specific behavior of the seed coat layer (8 μm) could be emphasized with this technique. It was shown that pulsed laser ablation could be a potential methodology to indirectly reveal wheat grain layer cohesion.

Lei et al. [68] reported on a pilot study to apply a calibration free (CF) LIBS approach for organic samples. The LIP was used to study the skin of a fresh potato, a typical root vegetable. The energy of the 266 nm, 5 ns ablation laser pulse was optimized in order to maintain the Local Thermodynamic Equilibrium (LTE) in LIP for the longest possible temporal interval. Due to the high sensitivity of the CF LIBS method to any discrepancy in LTE they concluded that the realistic plan for the application of the LIBS technique for fresh vegetables is to provide the measurements of relative concentrations of metallic trace and ultra-trace elements with respect to a reference element with a similar ionization potential, calcium or iron for example.

LIBS for space-resolved analysis of fresh vegetables was used by Juvé et al. [69]. Using a ns UV (266 nm) ablation laser the trace and ultra-trace element detection and qualitative analysis capabilities of LIBS analysis on fresh vegetables were demonstrated. Twenty seven trace elements have been identified in the LIBS spectra, including essential elements, metals and nonmetals. The group of Krug et al. [70,71] reported on the evaluation and optimization of LIBS for the determination of macro and micro-nutrients in plant samples. For the optimization of LIBS on pellets of plant samples, advanced statistical methods (Bayesian Regularized Artificial Neural Network approach) were employed. Using chemometric strategies, a single LIBS working experimental condition was proposed in order to maximize peak areas of several elements simultaneously. Experimental parameters such as integration time gate, time delay, number of pulses accumulated and detector amplification were investigated and optimized [70]. Recently [72], the sample preparation for plant analysis by LIBS, i.e. methods involving cryogenic grinding and planetary ball milling, were evaluated for leaves comminution before pellet preparation. The particle sizes were associated to chemical sample properties such as fiber and cellulose contents, as well as to pellet porosity and density. The pellets were ablated at 30 different sites by applying 25 laser pulses per site (Nd:YAG, 1064 nm, 5 ns, 10 Hz, 25 J cm^{-2}). Experiments carried out with pellets of sugarcane, orange tree and soy leaves showed that choosing the most appropriate grinding conditions had a significant affect on results for different plant species. There was up to 50% emission signal enhancement on LIBS measurements for most elements by improving particle size distribution and consequently the pellet porosity.

Periera et al. [73] uses LIBS combined with chemometrics to investigate the effect of bacteria *Candidatus Liberibacter asiaticus* (CLas) on citrus leaves. The inorganic and organic constituents of healthy and CLas-inoculated leaves were compared. The major, macro and micronutritiens were relevant for differentiating between healthy and infected plants. Predictive models worked out on the base of LIBS and chemometric analysis were applied to different inoculation times (from 1 to 8 months) and were effective in the classification of 82–97% of the diseased samples at the 95% significance level.

The use of ns and fs LIBS for the study of sunflower seedling (*Helianthus annuus* L.) stem samples was compared by Assion et al. [29]. Precise ablation conditions were found for the fs-laser, with a circular ablation zone and ablation depths below the thickness of the peripheral cell wall. Axial resolution of ~100 nm was reached. Samek et al. [74] compared the fs LIBS outcomes from measurements of Fe distribution on dried maize and fresh *Cornus stolonifera* leaves with the results of Relaxation Weighted Magnetic Resonance Imaging. The possibility to perform LIBS analysis of normal abundance of Fe in two leaf samples, which is as low as 5 ppm, was shown.

Fig. 1 demonstrates the LIBS capabilities for 2D high resolution mapping. Spatial distribution of elements is of great interest for plant biologists. To show the advantages of LIBS for this purpose, we aimed our attention at studying the effect of Pb treatment on spatial distribution of Mg in leaves of lettuce (Fig. 1A). Considering the fact that Mg is a key component of chlorophyll and Pb ions have a higher affinity to this complex, concentration of magnesium decreased in the leaf. One may suggest that concentration of Pb should increase, therefore, we analyzed leaves from maize plants treated with Pb ions and found that the concentration of Pb increased within the whole analyzed area (Fig. 1B). There are differences in the ability of plants to withstand toxic doses of metal ions, which is clearly indicated in Fig. 1C: it was found that Pb ion treatment did not cause any changes in concentration of Mg and, moreover, correlated well with the morphology of a plant leaf. Apart from leaves, LIBS can be used for determination of spatial element distribution on other

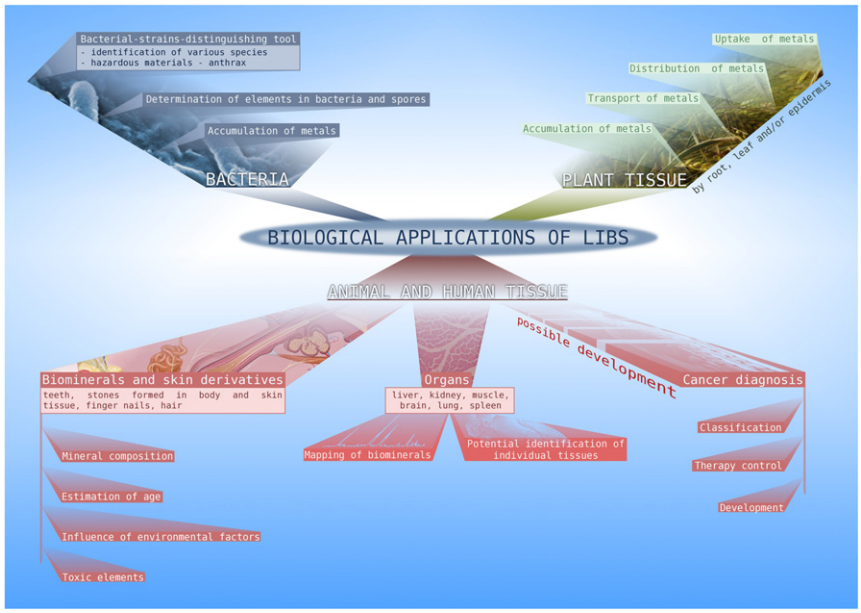

Fig. 1. Selected biological applications of LIBS. LIBS is used in the analysis of various kinds of bacteria, plant, human and animal tissues, skin derivatives, mapping of metals in tissues and analysis of biominerals. Recently, LIBS is considered as a potential tool for cancer diagnosis.

tissues such as pine branch (see Fig. 1D). The results were obtained by SP LIBS (Figs. 1A, B, and C) and/or by DP LIBS (Fig. 1D). The SP LIBS analysis was typically accomplished by using the second harmonic (532 nm) of a Nd:YAG laser system (Quantel, Brilliant B). The energy of the laser pulse on the sample plane was ~10 mJ per ~5 ns pulse duration. Ablation craters down to ~500 μm in diameter were created. The detection system consisted of a spectrometer (TRIAX 320, Jobin Yvon) in Czerny-Turner configuration with grating of 2400 groves/mm coupled to an ICCD detector (Jobin Yvon Horiba). The 277.98 nm Mg(I) and 405.78 nm Pb(I) lines, detected by gating the ICCD detector 1 μs after the laser pulse and with an observation window of 10 μs, were used for mapping. The DP LIBS measurement was realized in orthogonal configuration, using the 266 nm wavelength of the ablation laser (UP 266, New Wave, Macro) at energy 10 mJ per ~5 ns pulse and the 1064 nm radiation of the second laser (Quantel, Brilliant) at energy 100 mJ per ~6 ns pulse with an interpulse delay of 0.5 μs. This system allowed the creation of ablation craters for mapping down to ~100 μm in diameter. The same detection system as for the SP LIBS measurements was used. The 317.73 nm Ca(II) line detected 0.5 μs after the second laser pulse for a temporal interval 10 μs was utilized for creating the 3D distribution map. The LIBS analysis for all the measurements was performed in air at atmospheric pressure. The raw LIBS data are typically two-dimensional (2D) matrices of intensity values or peak areas derived from appropriate peak(s) detected for the given elements of interests.

3.4. LIBS for elemental mapping of biominerals

The group of biominerals analyzed with LIBS consists of teeth, bones and urinary stones [81]. LIBS can provide information on the distribution and contents of trace elements in these samples and help determine nutrition habits, conditions of growth, diseases and migration. LIBS and LIBS+LIFS techniques were used by Samek et al. [75,76] to study the presence of trace minerals in teeth and bones. A selection of teeth of different age groups ranging from the first teeth of infants, through the second teeth of children, to adults has been investigated quantitatively. The aim was to trace the influence of environmental factors on the accumulation of a number of elements in the teeth. A close link between elements detected in tooth fillings and toothpastes with those present in teeth was found. LIBS and LIFS were used in the analysis of important minerals and of toxic elements within the body. Samples from different parts of the body have been studied, including specimens of skin tissue, finger nails and teeth. Alvira et al. [84] applied an fs LIBS for characterization of Sr/Ca relative changes along incremental lines in enamel of human fossil and modern M3 teeth. They concluded that the employed instrumentation allows for the resolution of changes less than 5% of Sr/Ca ratio.

Cross-sectional study of kidney stones by LIBS is reported by Singh et al. [77]. A quantitative estimation of the Cu, Mg, Zn, and Sr trace element concentration is given in different parts of these stones. LIBS has proved to be a suitable method for obtaining the information about spatial distribution of elements in various kinds of stones found in the human body. Anzano and Lasheras [78] compared two strategies for the identification of urinary calculus by LIBS. As the first alternative, linear or parametric and rank or non-parametric correlation methods using μLIBS system were investigated. The second approach was based on the determination of elemental ratios of elements such as C, Ca, H, Mg, N, O, and P using a higher-energy laser system and an Echelle spectrograph.

Both methods and instrumentation have proven to be suitable for urinary-calculi identification. However, the second approach provided better analytical information about the analyzed sample.

The study on other type of biominerals, fossil bear teeth, bone and snake vertebra sections were reported by Galiova et al. [36,79] or Hrdlicka et al. [80]. LIBS, DP-LIBS and remote (standoff) LIBS similarly to LA-ICP-MS were proven to be suitable for fast, spatially resolved analyses of such calcified tissues. For the tooth section, in addition to microchemical analysis, the sample hardness was calculated using LIBS plasma ionic-to-atomic line intensity ratios of Mg (or Ca). In order to visualize non-destructively the fossil snake vertebra sample microstructure, X-ray microtomography was utilized.

3.5. LIBS for elemental mapping of products made from biological raw materials

Biological samples cover a broad field of materials. The definition of the biological sample is not simple if e.g. wood, skin or paper is also taken into account. Wood and wooden products are not the subject of this review. However, most interesting LIBS applications on paper, parchment and skin as less typical examples of the biological material selected here. Elemental distributions of paper and paper coatings were studied with excellent results when ArF (193 nm) and XeCl (308 nm) excimer lasers were used [81,82].The compositional mapping potential of LIBS in the analysis of coating coverage, coatweight distribution, and 3D distribution of various pigments of paper coating was described first in 1995 by Häkkänen and Korppi–Tommola [81]. They used a XeCl excimer laser source (308 nm) to generate the LIP. On areas typically $10 \times 10\ mm^2$ at a spatial resolution of 250 μm the Si and Ca distribution was measured. With a single laser pulse (0.2 mJ of energy), about 2 ng of coating from a volume of 30 μm in diameter and 2 μm in depth was vaporized. Dolgin et al. [83] used LIBS for rapid characterization of parchment. Distinction between modern and historical samples was achieved by discriminant analysis of the LIBS data using the signals from the elements Ca, Na, K, Fe, and Mn. Animal type recognition was also possible on the basis of Mg/Cu emission peak ratio and Mg depth profiling. The LIBS results were compared with results from ICP-MS and a good correlation was obtained. Sun et al. [84,85] evaluated the effectiveness of skin protection creams against the zinc ion absorption from aqueous zinc chloride solution and oil paste of zinc oxide by measuring the depth profile of Zn signal (zinc atomic emission line at 213.9 nm) within the skin. A Nd:YAG laser at 1064 nm was used with a pulse energy of 100 mJ. The experimental results indicated that Zn was absorbed through the skin and the concentration decreased exponentially with the skin depth. Taschuk et al. [86] reported another example close to skin analysis. LIBS mapping in forensic science was shown through the detection of latent fingerprints on a Si wafer by LIBS using approximately 120 fs pulses at 400 nm with energies of (84 ± 7) μJ. The presence of a fingerprint ridge is found by observing the Na emission lines from the transferred skin oil. The presence of the thin layer of transferred oil was also found to be sufficient to suppress the LIBS signal from the Si substrate, giving an alternative method of mapping the latent fingerprint using the Si emission. A two-dimensional image of a latent fingerprint can be successfully collected using these techniques. Since then, many various applications of LIBS were reported including certain biological applications as shown in Fig. 2.

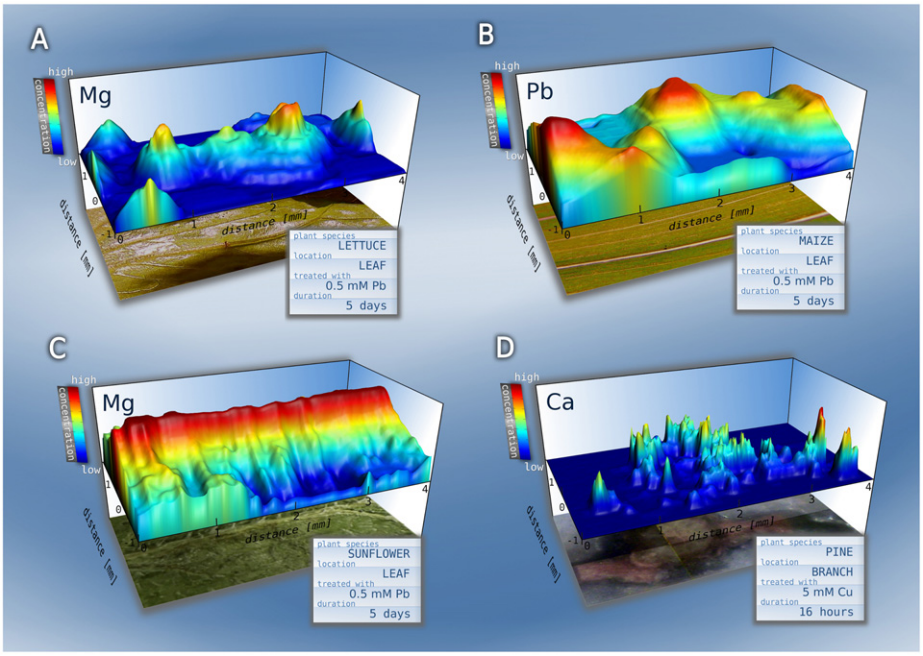

Fig. 2. Use of 3D modeling for visualization of measured data obtained by single-shot (SP) LIBS analysis of (A) lettuce, (B) maize and (C) sunflower leaves treated with Pb(II) ions and by (D) DP LIBS analysis of branch slice of pine treated with Cu(II) ions.

4. Conclusions

LIBS as a sensitive optical technique capable of fast multi-elemental analysis proved to be a versatile tool in different applications. Among others, the main advantages are minimum sample preparation for analysis and the possibility of spatially resolved analysis from discrete points with instantaneous detection of the microplasma emission. In this article, the utilization of LIBS for trace elemental analysis in different matrices is reviewed and the applicability of LIBS to trace metal mapping in biological samples is emphasized. The theory of LIBS is briefly discussed as well as a variety of instruments and their components thoroughly and systematically reviewed. Furthermore a comprehensive review of the applications of LIBS is reported in this article.

Besides review of the technical aspects and current applications, the expected future directions need to be discussed. Together with the trace element mapping in tissues, which is of great and increasing interest to many biologists, biochemists and clinicians, spatial distribution of metal-based drugs can be a topic of future targeted research. In tissue, there is no presence of platinum derivatives which are still the most commonly used anti-cancer drugs worldwide. The spatial distribution of this metal in tumors can reveal new findings including the inner mechanisms of a tumor that metabolizes the drug, how to transport it within tumor tissue and how to defend itself against the adverse effects. This particular application of LIBS has not yet been realized, but its potential is very high.

Acknowledgments

This work was supported by the grants ME09015 and MSM0021622411 of the Ministry of Education of the Czech Republic and by the project "CEITEC—Central European Institute of Technology" (CZ.1.05/1.1.00/02.0068) from European Regional Development Fund. Research at Oak Ridge National Laboratory was supported by the US Department of Energy (DOE), Office of Science, Biological and Environmental Research program through the Consortium for Carbon Sequestration in Terrestrial Ecosystems. Oak Ridge National Laboratory is managed by UT-Battelle, LLC, for the DOE under Contract DEAC05-00OR22725. The authors also wish to express their thanks for financial support to NANIMEL GA CR 102/08/1546. Moreover, the authors thank very much to Lucie Krajcarova, Pavlina Sobrova and Petr Koudelka for excellent technical assistance.

References

[1] D.A. Cremers, L.J. Radziemski, Handbook of Laser-Induced Breakdown Spectroscopy, Wiley & Sons, Chichester, 2006.
[2] A. Miziolek, V. Palleschi, I. Schecter, Laser-Induced Breakdown Spectroscopy (LIBS) Fundamentals and Applications, Cambridge University Press, New York, 2006.
[3] J.P. Singh, S.N. Thakur, Laser-Induced Breakdown Spectroscopy, Amsterdam, 2007.
[4] F. Brech, L. Cross, Applied Spectroscopy 16 (1962) 59.
[5] J. Debras-Guedon, N. Liodec, Comptes Rendus Hebdomadaires des Seances de I' Academie des Sciences 257 (1963) 3336–3339.
[6] K.G. Snetsing, K. Keil, American Minerologist 52 (1967) 1842–1854.
[7] W.W. Schroede, J.J. Vannieke, L. Dicks, A. Strashei H.V.D. Peipen, Spectrochimica Acta Part B-Atomic Spectroscopy 26 (1971) 331–340.
[8] T.R. Loree, L.J. Radziemski, Plasma Chemistry and Plasma Processing 1 (1981) 271–280.
[9] L.J. Radziemski, T.R. Loree, Plasma Chemistry and Plasma Processing 1 (1981) 281–293.
[10] E. Tognoni, V. Palleschi, M. Corsi, G. Cristoforetti, Spectrochimica Acta Part B-Atomic Spectroscopy 57 (2002) 1115–1130.
[11] C. Pasquini, J. Cortez, L.M.C. Silva, F.B. Gonzaga, Journal of the Brazilian Chemical Society 18 (2007) 463–512.
[12] E. Tognoni, G. Cristoforetti, S. Legnaioli, V. Palleschi, Spectrochimica Acta Part B-Atomic Spectroscopy 65 (2010) 1–14.
[13] L. Xian-Yun, Z. Wei-Jun, Journal of Biomedical Science and Engineering 1 (2008) 147–151.
[14] D.A. Cremers, R.C. Chinni, Applied Spectroscopy Reviews 44 (2009) 457–506.
[15] R. Gaudiuso, M. Dell'Aglio, O. De Pascale, G.S. Senesi, A. De Giacomo, Sensors 10 (2010) 7434–7468.
[16] A.A. Bol'shakov, J.H. Yoo, C.Y. Liu, J.R. Plumer, R.E. Russo, Applied Optics 49 (2010) C132–C142.
[17] R.E. Russo, X.L. Mao, H.C. Liu, J. Gonzalez, S.S. Mao, Talanta 57 (2002) 425–451.
[18] J.D. Winefordner, I.B. Gornushkin, T. Correll, E. Gibb, B.W. Smith, N. Omenetto, Journal of Analytical Atomic Spectrometry 19 (2004) 1061–1083.
[19] K. Novotny, J. Kaiser, M. Galiova, V. Konecna, J. Novotny, R. Malina, M. Liska, V. Kanicky, V. Otruba, Spectrochimica Acta Part B-Atomic Spectroscopy. 63 (2008) 1139–1144.
[20] C. Latkoczy, T. Ghislain, Journal of Analytical Atomic Spectrometry 21 (2006) 1152–1160.
[21] M. Senoner, T. Wirth, W.E.S. Unger, Journal of Analytical Atomic Spectrometry 25 (2010) 1440–1452.
[22] H. Bette, R. Noll, Journal of Physics D-Applied Physics 37 (2004) 1281–1288.
[23] V. Piscitelli, J. Gonzalez, X.L. Mao, A. Fernandez, R. Russo, in: N.U. Wetter, J. Frejlich (Eds.), Riao/Optilas 2007, Melville, 2008, pp. 1166–1171.
[24] R.E. Russo, T.W. Suen, A.A. Bol'shakov, J. Yoo, O. Sorkhabi, X.L. Mao, J. Gonzalez, D. Oropeza, V. Zorba, Journal of Analytical Atomic Spectrometry 26 (2011) 1596–1603.
[25] J.S. Becker, International Journal of Mass Spectrometry 289 (2010) 65–75.
[26] J.S. Becker, M. Zoriy, A. Matusch, B. Wu, D. Salber, C. Palm, Mass Spectrometry Review 29 (2010) 156–175.
[27] T. Kim, C.T. Lin, Y. Yoon, Journal of Physics Chemistry B 102 (1998) 4284–4287.
[28] C. Petibois, M.C. Guidi, Analytical and Bioanalytical Chemistry 391 (2008) 1599–1608.
[29] A. Assion, M. Wollenhaupt, L. Haag, F. Mayorov, C. Sarpe-Tudoran, M. Winter, U. Kutschera, T. Baumert, Applied Physics B-Lasers and Optics 77 (2003) 391–397.
[30] Z.Y. Qin, J.A. Caruso, B. Lai, A. Matusch, J.S. Becker, Metallomics 3 (2011) 28–37.
[31] J. Kalvoda, M. Novak, O. Babek, R. Brzobohaty, M. Hola, I. Holoubek, V. Kanicky, R. Skoda, Biogeochemistry 94 (2009) 197–215.
[32] S. Taira, Y. Sugiura, S. Moritake, S. Shimma, Y. Ichiyanagi, M. Setou, Analytical Chemistry 80 (2008) 4761–4766.

[33] S.G. Buckley, G.A. Lithgow, C.B. Stipe, LIBS in Industry: Sparks Fly, Tucson, AZ, USA, Optical Society of America: OSA Technical Digest (CD), 2010, Paper AMC1.
[34] A. De Giacomo, M. Dell'Aglio, D. Bruno, R. Gaudiuso, O. De Pascale, Spectrochimica Acta Part B-Atomic Spectroscopy 63 (2008) 805–816.
[35] V.I. Babushok, F.C. DeLucia, J.L. Gottfried, C.A. Munson, A.W. Miziolek, Spectrochimica Acta Part B-Atomic Spectroscopy 61 (2006) 999–1014.
[36] M. Galiova, et al., Applied Optics 49 (2010) C191–C199.
[37] S. Laville, C. Goueguel, H. Loudyi, F. Vidal, M. Chaker, M. Sabsabi, Spectrochimica Acta Part B-Atomic Spectroscopy 64 (2009) 347–353.
[38] J. Le Meur, D. Menut, P. Wodling, L. Salmon, P.Y. Thro, S. Chevillard, N. Ugolin, Spectrochimica Acta Part B-Atomic Spectroscopy 63 (2008) 465–473.
[39] S. Morel, N. Leone, P. Adam, J. Amouroux, Applied Optics 42 (2003) 6184–6191.
[40] A.C. Samuels, F.C. DeLucia, K.L. McNesby, A.W. Miziolek, Applied Optics 42 (2003) 6205–6209.
[41] T. Kim, Z.G. Specht, P.S. Vary, C.T. Lin, Journal of Physical Chemistry B 108 (2004) 5477–5482.
[42] M. Baudelet, L. Guyon, J. Yu, J.P. Wolf, T. Amodeo, E. Frejafon, P. Laloi, Journal of Applied Physics 99 (2006) 1–9.
[43] M. Baudelet, L. Guyon, J. Yu, J.P. Wolf, T. Amodeo, E. Frejafon, P. Laloi, Applied Physics Letters 88 (2006) 1–3.
[44] M. Baudelet, J. Yu, M. Bossu, J. Jovelet, J.P. Wolf, T. Amodeo, E. Frejafon, P. Laloi, Applied Physics Letters 89 (2006) 1–3.
[45] J. Diedrich, S.J. Rehse, S. Palchaudhuri, Journal of Applied Physics 102 (2007) 1–8.
[46] J. Diedrich, S.J. Rehse, S. Palchaudhuri, Applied Physics Letters 90 (2007) 1–3.
[47] S.J. Rehse, J. Diedrich, S. Palchaudhuri, Spectrochimica Acta Part B-Atomic Spectroscopy 62 (2007) 1169–1176.
[48] S.J. Rehse, N. Jeyasingham, J. Diedrich, S. Palchaudhuri, Journal of Applied Physics 105 (2009) 1–13.
[49] S.J. Rehse, Q.I. Mohaidat, S. Palchaudhuri, Applied Optics 49 (2010) C27–C35.
[50] R.A. Multari, D.A. Cremers, J.M. Dupre, J.E. Gustafson, Applied Spectroscopy 64 (2010) 750–759.
[51] J.L. Gottfried, F.C. De Lucia, C.A. Munson, A.W. Miziolek, Spectrochimica Acta Part B-Atomic Spectroscopy 62 (2007) 1405–1411.
[52] J.L. Gottfried, F.C. De Lucia, C.A. Munson, A.W. Miziolek, Applied Spectroscopy 62 (2008) 353–363.
[53] A.P.M. Michel, Spectrochimica Acta Part B-Atomic Spectroscopy 65 (2010) 185–191.
[54] A. Kumar, F.Y. Yueh, J.P. Singh, S. Burgess, Applied Optics 43 (2004) 5399–5403.
[55] A. El-Hussein, A.K. Kassem, H. Ismail, M.A. Haritha, Talanta 82 (2010) 495–501.
[56] M.J. Myers, J.D. Myers, B.P. Guo, C.X. Yang, C.R. Hardy, J.A. Myers, A.G. Myers, S.M. Christian, in: G.L. Cote, A.V. Priezzhev (Eds.), Optical Diagnostics and Sensing Viii, Bellingham, 2008, p. W8630 W8630.
[57] D. Santos, R.E. Samad, L.C. Trevizan, A.Z. de Freitas, N.D. Vieira, F.J. Krug, Applied Spectroscopy 62 (2008) 1137–1143.
[58] F.Y. Yueh, H.B. Zheng, J.P. Singh, S. Burgess, Spectrochimica Acta Part B-Atomic Spectroscopy 64 (2009) 1059–1067.
[59] E. Lombi, K.G. Scheckel, I.M. Kempson, Environmental and Experimental Botany 72 (2011) SI 13–17.
[60] M.Z. Martin, N. Labbe, N. Andre, R. Harris, M. Ebinger, S.D. Wullschleger, A.A. Vass, Spectrochimica Acta Part B-Atomic Spectroscopy 62 (2007) 1426–1432.
[61] M.Z. Martin, A.J. Stewart, K.D. Gwinn, J.C. Waller, Applied Optics 49 (2010) C161–C167.
[62] M. Galiova, et al., Spectrochimica Acta Part B-Atomic Spectroscopy 62 (2007) 1597–1605.
[63] M. Galiova, J. Kaiser, K. Novotny, J. Novotny, T. Vaculovic, M. Liska, R. Malina, K. Stejskal, V. Adam, R. Kizek, Applied Physics A-Materials Science and Processing 93 (2008) 917–922.
[64] J. Kaiser, et al., Spectrochimica Acta Part B-Atomic Spectroscopy 64 (2009) 67–73.
[65] S. Krizkova, et al., Sensors 8 (2008) 445–463.
[66] M. Galiova, J. Kaiser, K. Novotny, M. Hartl, R. Kizek, P. Babula, Microscopic Research and Technique 74 (2011) 845–852.
[67] M.R. Martelli, C. Barron, P. Delaporte, G. Viennois, X. Rouau, A. Sadoudi, Journal of Cereal Science 49 (2009) 354–362.
[68] W.Q. Lei, V. Motto-Ros, M. Boueri, Q.L. Ma, D.C. Zhang, L.J. Zheng, H.P. Zeng, J. Yu, Spectrochimica Acta Part B-Atomic Spectroscopy 64 (2009) 891–898.
[69] V. Juve, R. Portelli, M. Boueri, M. Baudelet, J. Yu, Spectrochimica Acta Part B-Atomic Spectroscopy 63 (2008) 1047–1053.
[70] L.C. Nunes, G.A. da Silva, L.C. Trevizan, D. Santos, R.J. Poppi, F.J. Krug, Spectrochimica Acta Part B-Atomic Spectroscopy 64 (2009) 565–572.
[71] L.C. Trevizan, D. Santos, R.E. Samad, N.D. Vieira, L.C. Nunes, I.A. Rufini, F.J. Krug, Spectrochimica Acta Part B-Atomic Spectroscopy 64 (2009) 369–377.
[72] M.S. Gomes, D. Santos, L.C. Nunes, G. Gustinelli, A. Carvalho, F.O. Leme, F.J. Krug, Talanta 85 (2011) 1744–1750.
[73] F.M.V. Pereira, D.M.B.P. Milori, A.L. Venancio, M.S.T. Russo, P.K. Martins, J. Freitas-Astua, Talanta 83 (2010) 351–356.
[74] O. Samek, J. Lambert, R. Hergenroder, M. Liska, J. Kaiser, K. Novotny, S. Kukhlevsky, Laser Physics Letters 3 (2006) 21–25.
[75] O. Samek, D.C.S. Beddows, H.H. Telle, G.W. Morris, M. Liska, J. Kaiser, Applied Physics A-Materials Science and Processing 69 (1999) S179–S182.
[76] O. Samek, M. Liska, J. Kaiser, V. Krzyzanek, D.C.S. Beddows, A. Belenkevitch, G.W. Morris, H.H. Telle, in: F. Baldini, N.I. Croitoru, M. Frenz, I. Lundstrom, M. Miyagi, R. Pratesi, O.S. Wolfbeis (Eds.), Proceedings of the Biomedical Sensors, Fibers, and Optical Delivery Systems, Bellingham, 1999, pp. 263–271.
[77] V.K. Singh, A.K. Rai, P.K. Rai, P.K. Jindal, Lasers in Medical Science 24 (2009) 749–759.
[78] J. Anzano, R.J. Lasheras, Talanta 79 (2009) 352–360.
[79] M. Galiova, J. Kaiser, K. Novotny, M. Ivanov, M. Nyvltova-Fisakova, L. Mancini, G. Tromba, T. Vaculovic, M. Liska, V. Kanicky, Analytical and Bioanalytical Chemistry 398 (2010) 1095–1107.
[80] A. Hrdlicka, et al., Applied Optics 49 (2010) C16–C20.
[81] H.J. Hakkanen, J.E.I. Korppi-Tommola, Applied Spectroscopy 49 (1995) 1721–1728.
[82] H. Hakkanen, J. Houni, S. Kaski, J.E.I. Korppi-Tommola, Spectrochimica Acta Part B-Atomic Spectroscopy 56 (2001) 737–742.
[83] B. Dolgin, Y.H. Chen, V. Bulatov, I. Schechter, Analytical and Bioanalytical Chemistry 386 (2006) 1535–1541.
[84] Q. Sun, M. Tran, B. Smith, J.D. Winefordner, Contact Dermatitis 43 (2000) 259–263.
[85] Q. Sun, M. Tran, B.W. Smith, J.D. Winefordner, Talanta 52 (2000) 293–300.
[86] M.T. Taschuk, Y.Y. Tsui, R. Fedosejevs, Applied Spectroscopy 60 (2006) 1322–1327.